# The radical-binding lipocalin A1M binds to a Complex I subunit and protects mitochondrial structure and function.

Gram, Magnus; Wester Rosenlöf, Lena; Kotarsky, Heike; Olofsson, Tor; Leanderson, Tomas; Mörgelin, Matthias; Fellman, Vineta; Åkerström, Bo

*Published in:*
Antioxidants & Redox Signaling

*DOI:*
10.1089/ars.2012.4658

2013

ANTIOXIDANTS & REDOX SIGNALING
Volume 18, Number 16, 2013

DOI: 10.1089/ars.2012.4658

Discoveries

ORIGINAL RESEARCH COMMUNICATION

# The Radical-Binding Lipocalin A1M Binds to a Complex I Subunit and Protects Mitochondrial Structure and Function

Magnus G. Olsson,[1] Lena W. Rosenlöf,[1] Heike Kotarsky,[2] Tor Olofsson,[3] Tomas Leanderson,[4] Matthias Mörgelin,[1] Vineta Fellman,[2,5,6] and Bo Åkerström[1]

## Abstract

***Aims:*** During cell death, energy-consuming cell degradation and recycling programs are performed. Maintenance of energy delivery during cell death is therefore crucial, but the mechanisms to keep the mitochondrial functions intact during these processes are poorly understood. We have investigated the hypothesis that the heme- and radical-binding ubiquitous protein $\alpha_1$-microglobulin (A1M) is involved in protection of the mitochondria against oxidative insult during cell death. ***Results:*** Using blood cells, keratinocytes, and liver cells, we show that A1M binds with high affinity to apoptosis-induced cells and is localized to mitochondria. The mitochondrial Complex I subunit NDUFAB1 was identified as a major molecular target of the A1M binding. Furthermore, A1M was shown to inhibit the swelling of mitochondria, and to reverse the severely abrogated ATP-production of mitochondria when exposed to heme and reactive oxygen species (ROS). ***Innovation:*** Import of the radical- and heme-binding protein A1M from the extracellular compartment confers protection of the mitochondrial structure and function during cellular insult. ***Conclusion:*** A1M binds to a subunit of Complex I and has a role in assisting the mitochondria to maintain its energy delivery during cell death. A1M may also, at the same time, counteract and eliminate the ROS generated by the mitochondrial respiration to prevent oxidative damage to surrounding healthy tissue. *Antioxid. Redox Signal.* 18, 2017–2028.

## Introduction

The term oxidative stress is used to describe conditions with an abnormally high production of redox-active compounds or impaired antioxidative tissue defense systems (17). Reactive oxygen species (ROS) are highly reactive compounds and include both hydrogen peroxide ($H_2O_2$) and the free radicals hydroxyl ($^{\cdot}OH$) and superoxide ($O_2^{\cdot -}$). Important generators of ROS are hemoglobin (Hb), released from red blood cells during hemorrhage and hemolytic conditions, and its prosthetic group, iron-containing heme (10). ROS induce oxidative stress by undergoing redox reactions with cellular and extracellular molecular components, leading to covalent modifications of DNA, membrane lipids, and proteins and a subsequent loss of function.

Under normal circumstances, the adverse effects of ROS are counteracted by antioxidants such as the enzymes superoxide dismutase, catalase, and glutathione peroxidases. Recently, a novel endogenous antioxidant, the lipocalin and radical-binding protein $\alpha_1$-microglobulin (A1M), has been described to protect cells and matrix fibrils from Hb-, heme- and ROS-induced oxidative damage (28, 33, 36, 37). A1M is a reductase (2), a binder of heme groups (1d, 22), and a multispecific scavenger of small organic radicals (1c). It is a 26-kDa plasma and tissue protein (1b) mainly synthesized in the liver (45) and in less amounts in peripheral organs (4, 20). A1M is found in

**Innovation**

Import of the radical- and heme-binding protein $\alpha_1$-microglobulin from the extracellular compartment confers protection of mitochondrial structure and function against oxidative stress during cellular insult.

Divisions of [1]Infection Medicine, [2]Pediatrics, [3]Hematology and Transfusion Medicine and [4]Immunology, Lund University, Lund, Sweden.
[5]Children's Hospital, Helsinki University Hospital, University of Helsinki, Helsinki, Finland.
[6]Folkhälsan Research Center, Helsinki, Finland.

the blood at 1–2 $\mu M$ (5, 8) and is rapidly distributed to the extravascular compartments (23). Adding to the antioxidation properties, an increased synthesis in the liver, blood cells, placenta, and skin keratinocytes is induced by cell-free Hb and ROS (28, 32, 34, 35).

Cell death, whether accidental, stress-induced, or apoptotic, frequently involves activation of cell degradation and recycling programs (7). Therefore, cell death is an energy-depending process in need of preserved and intact mitochondrial functions. Furthermore, cell death *in vivo* is associated with generation of redox-active compounds, and the dying cells need to protect themselves and surrounding tissue from oxidative damage. Mitochondria are generally regarded as a major source of ROS, and autophagocytic elimination of mitochondria (mitophagy) is suggested to play a central role during programmed cell death (24). Thus, there is a need of protection from oxidative stress generated by mitochondria and other sources, on one hand, and a need of functional mitochondria, on the other, during programmed cell death, and it is not yet understood how this is accomplished. We hypothesized that enhanced antioxidation activity may play a pivotal role and therefore investigated a possible association of A1M to intracellular structures during cell death. Here, we have found evidence of a specific binding of A1M to a subunit of Complex I, localizing A1M to mitochondria. The results also indicate that this localization confers protection of the mitochondrial structure and function during fatal oxidative insult toward the cell.

## Results

### *Specific binding of A1M to damaged cells*

Binding of A1M to apoptotic and healthy cells was analyzed by flow cytometry and compared to untreated cells. First, apoptosis was induced in murine T-cell hybridomas (HCQ.4) by cross-linking of the CD3 molecule with immobilized anti-mouse CD3 antibodies (Fig. 1A, E), or by incubation with 5% ethanol or 10% dimethyl sulfoxide (DMSO) (Fig. 1B). These treatments resulted in DNA fragmentation and uptake of trypan blue after 15–18 h (not shown). A weak binding of A1M could be detected to untreated cells (Fig. 1A, left panel). An additional stronger binding was detected to cells cross-linked with anti-CD3 (Fig. 1A, right panel) or treated with ethanol or DMSO (Fig. 1B). The binding could be correlated to propidium iodide (PI) uptake; that is, only cells that could incorporate PI displayed the stronger binding of A1M (Fig. 1B). Flow cytometry of a murine pre-B-cell line (70Z/3), induced to apoptosis using the benzamide drug declopramide (3-CPA) and incubated with A1M followed by anti-A1M, showed similar results (Fig. 1C), indicating that the binding to apoptotic cells is not restricted to T cells.

To further characterize the A1M binding to damaged cells, the binding was also studied using fluorescence and confocal microscopy of the human erythroid cell line (K562) (Fig. 1D) and the promyelocytic cell line HL 60 (not shown) exposed to heme, and incubated with A1M followed by anti-A1M. Two different types of staining could be seen: a pronounced, intracellular, and uniform staining to a subset ($\sim$6%) of the cells (confocal microscopy, Fig. 1D), and a weak granular staining to the cell surface of most cells (fluorescence microscopy, not shown). Similar results were obtained with the HL 60 cells. These results indicate that the strong binding of A1M to damaged cells is mainly intracellular.

To investigate the specificity of the binding, a competitive cell-binding assay was performed on HCQ.4 cells, induced to apoptosis by CD3 cross-linking, and compared to normal untreated cells. $^{125}$I-labeled A1M and an excess of unlabeled A1M, ovalbumin, bovine serum albumin (BSA), or $\alpha_1$-acid glycoprotein (AGP) were added to the cells (Fig. 1E). More A1M was bound to apoptotic cells (Fig. 1E, right) compared to untreated cells (left). Excess of unlabeled A1M blocked the $^{125}$I-A1M binding to the same basal level for apoptotic cells as for untreated cells. The reduction was found to be significant ($p < 0.001$). None of the unlabeled control proteins could significantly reduce the binding of $^{125}$I-A1M to untreated cells, thus indicating a specific binding of A1M. To the apoptotic cells, there was a small, significant reduction by the control proteins ($p < 0.05$). This small reduction may be due to an increased unspecific background binding to exposed intracellular structures. Accordingly, the results indicate a specific strong binding of A1M to apoptotic cells. From a Scatchard plot, an affinity constant for the A1M binding to apoptotic HCQ.4 cells could be determined to $1 \times 10^6\ M^{-1}$. The viability of these cells was 25% according to trypan blue exclusion.

As mentioned above, the A1M-binding cells internalized PI (Fig. 1B). This indicates that the A1M-binding occurred late in the apoptotic process after the cell membranes start to leak. To confirm this result, time studies on the binding of A1M to HCQ.4 cells, induced to apoptosis by anti-CD3 cross-linking, were performed. Flow cytometry of samples taken at various timepoints after induction shows that the PI uptake precedes the binding of A1M (Fig. 2A). This correlation was not seen to cells negative for PI uptake. The same result was obtained when the 70Z/3 were triple-stained with A1M, annexin V (marker for apoptosis), and 7-amino actinomycin D (7AAD, marker dye for cell membrane permeability) (Fig. 2B). Only 7AAD-positive cells showed a strong A1M binding, whereas cells positive for annexin V, but not for 7AAD, did not bind A1M.

### *Identification of intracellular A1M-binding proteins*

To search for cellular proteins interacting with A1M, the yeast 2-hybrid system was used. cDNA coding for A1M was used as a bait to search for A1M-interacting proteins in a human leukocyte library. Approximately $2 \times 10^6$ transformants were analyzed for reporter gene activation. A total of 168 colonies survived on plates lacking histidine, and 13 of them were also positive for $\beta$-galactosidase. The $His^+LacZ^+$ recombinant library plasmids were isolated and tested in direct two-hybrid assays with bait plasmids encoding only the bait protein as well as the protein fused to unrelated proteins. Eleven recombinant plasmids were shown to encode proteins that interacted with A1M, but not with the bait protein or other unrelated proteins fused to it. DNA sequencing of the inserts revealed that seven of them were a truncated form of the SDAP subunit (NDUFAB1) in mitochondrial Complex I; one was the complete sequence of the same subunit; one was a small nuclear RNA (snRNA)-binding protein; one was *N*-acetylglucosamine kinase; and one was a colon cancer antigen. All inserts were in frame in the prey vector (Table 1).

### *Binding of A1M to mitochondrial Complex I*

The results from the yeast two-hybrid experiments thus suggest that a subunit of mitochondrial Complex I is a major

A1M-binding intracellular protein. Binding to mitochondria and to Complex I, in particular, was therefore investigated in detail using several independent methods: confocal microscopy, electron microscopy, subcellular fractionation, and polyacrylamide gel electrophoresis (PAGE). Using a mitochondrial fluorescent probe (MitoTracker) and confocal microscopy, we evaluated the subcellular localization of the intracellular A1M in K562 cells with or without addition of exogenous A1M (Fig. 3A). Analyzing cells without exogenously added A1M, a very weak unspecific intracellular staining was observed (not shown). However, with the addition of exogenous A1M, an intense, mitochondrial-specific staining was observed. The subcellular localization of the bound A1M was also studied by transmission electron microscopy (TEM) using primary human keratinocyte cultures

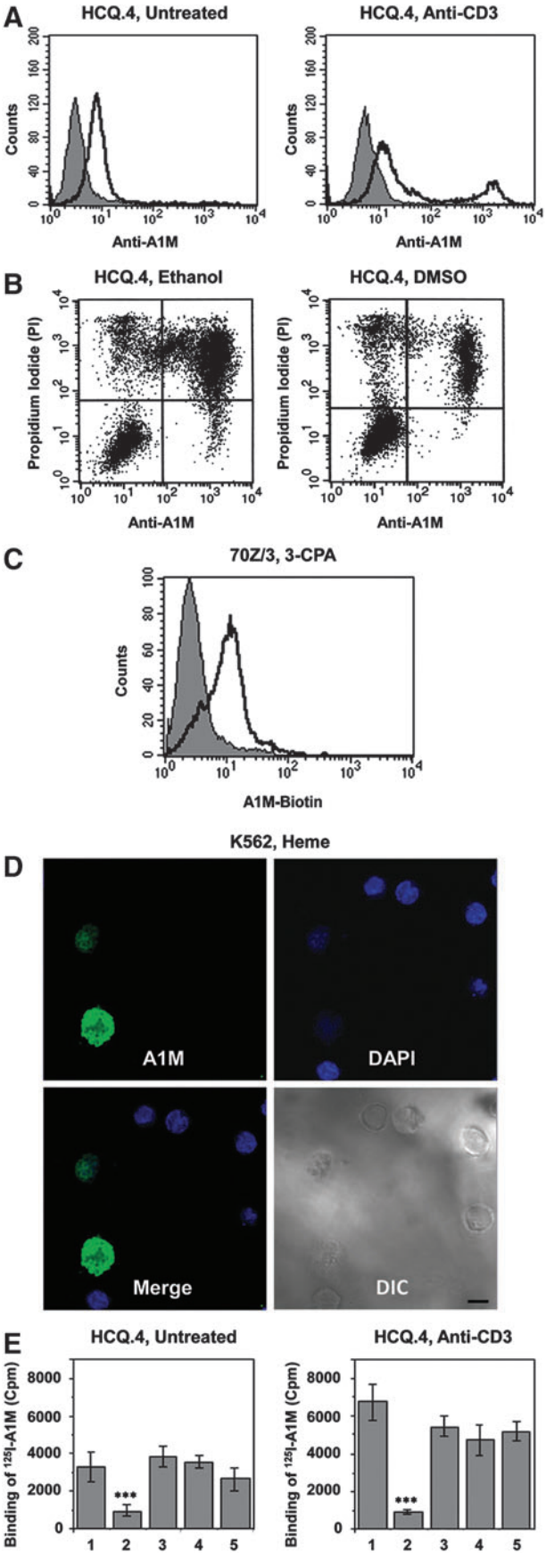


**FIG. 1. Binding of $\alpha_1$-microglobulin (A1M) to intact and apoptotic cells. (A)** Murine T-cell hybridoma cell line (HCQ.4) cells were cultured on hamster anti-mouse CD3 antibody- (4 $\mu$g/ml) coated plastics for 18 h. For analysis of A1M binding, $1\times10^6$ cells were incubated with 1 mg/ml A1M, washed, incubated with mouse anti-A1M antibodies, washed, and finally incubated with FITC-conjugated goat anti-mouse IgG (GAM-FITC). About 10,000 cells were analyzed for A1M binding (open peak). Background was set by cells incubated with bovine serum albumin (BSA) in the first step (shaded peak). Binding to apoptotic cells (right histogram) was compared to untreated cells (left histogram). **(B)** The binding of A1M was correlated to the uptake of PI by culturing HCQ.4 cells in the presence of 5% ethanol or 10% dimethyl sulfoxide (DMSO) for 15 h. For the flow cytometry analysis, A1M was incubated with cells, followed by mouse anti-A1M antibodies, and FITC-conjugated goat anti-mouse IgG. Before analysis, cells were also stained by propidium iodide (PI) to detect dead cells. **(C)** Binding of A1M to apoptotic cells of the pre-B-cell line 70Z/3 was analyzed by flow cytometry. The cells were induced to apoptosis by the benzamide drug declopramide (3-CPA) for 15 h and analyzed for A1M binding by incubation of biotinylated A1M, followed by SAPE. The background was set by cells incubated with SAPE only (shaded peak). **(D)** K562 cells were incubated with 20 $\mu M$ heme and 0.25 mg/ml A1M for 2 h and subjected to staining with mouse anti-A1M antibodies (23.26) followed by goat anti-mouse IgG F(ab')$_2$ fragments (Alexa Fluor® 488; green). Cells were mounted using ProLong Gold AntiFade Reagent with 4'-6-diamidino-2-phenylindole (DAPI; blue). Analyses were performed using epifluorescence microscopy and confocal microscopy as described in the Materials and Methods section. Cellular morphology was determined using differential interference contrast (DIC). The picture is a representative for three separate experiments. Size bar is 10 $\mu$m. **(E)** The specificity of the A1M binding was determined by a competitive cell-binding assay. HCQ.4 cells, induced to apoptosis by cross-linking with anti-CD3 for 18 h (right histogram), were compared to untreated HCQ.4 cells (left histogram). About $1\times10^6$ cells/sample were mixed with 1 $\mu$g/ml of $^{125}$I-A1M (1), $^{125}$I-A1M plus addition of 2.5 mg/ml of unlabeled A1M (2), ovalbumin (3), BSA (4), or AGP (5). The cells were incubated for 30 min at 4°C, centrifuged on a sucrose gradient to separate unbound protein, and tubes were then frozen, and the cell pellet was cut off and counted in a $\gamma$-counter. The results are presented as mean values of a triplicate from one experiment ± SEM. Groups were statistically compared using Student's *t*-test. ***$p<0.001$.

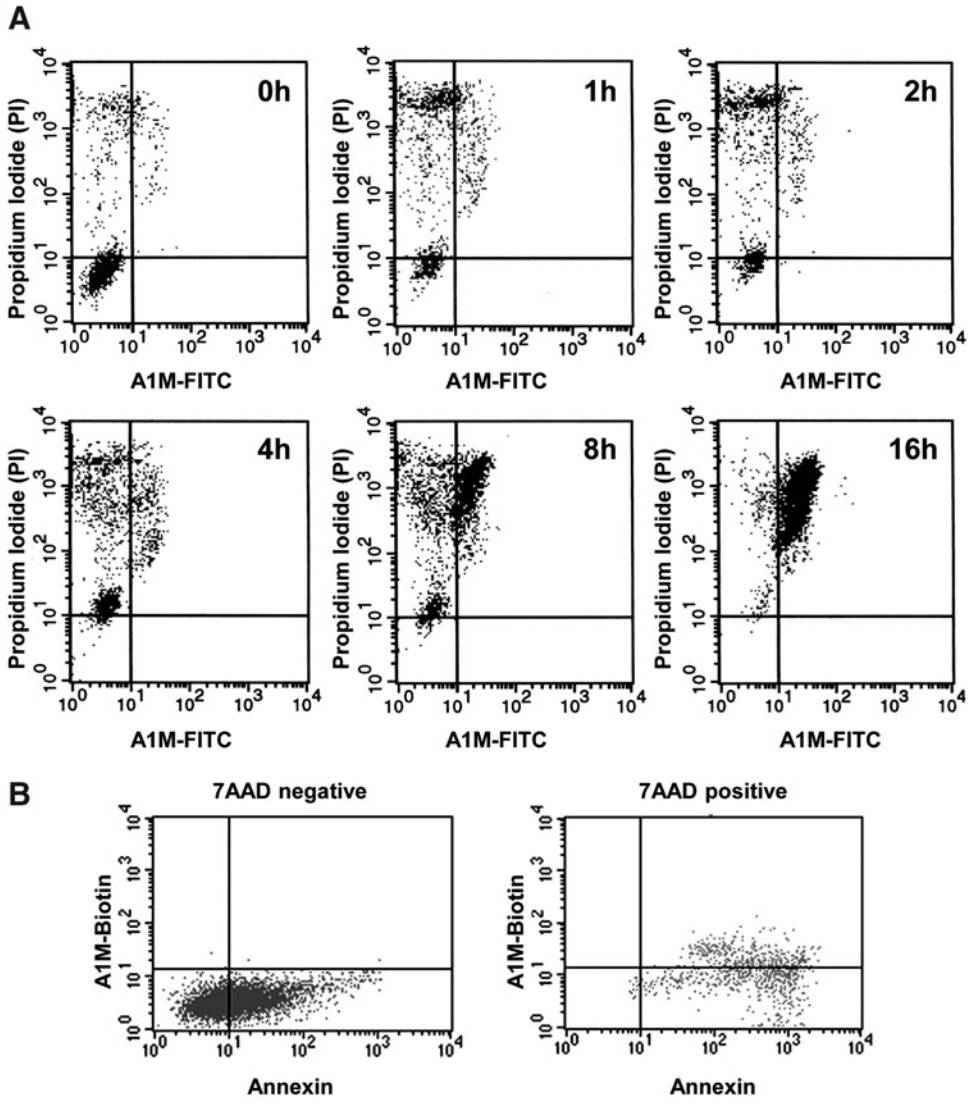


**FIG. 2. Time studies of the binding of A1M to apoptotic cells. (A)** Apoptosis was induced in HCQ.4 cells by cultivation on anti-CD3-coated plastics. Samples were taken at different timepoints after induction (0, 1, 2, 4, 8, and 16 h). The cells were stained with FITC-conjugated A1M (0.1 mg/ml) and PI. About 10,000 cells were analyzed. **(B).** Binding of A1M to pre-B-cells, induced to apoptosis by incubation with the benzamide 3-CPA, was analyzed by flow cytometry and correlated to binding of annexin V and 7AAD uptake. The apoptotic 70Z/3 cells were incubated with biotinylated A1M (0.025 mg/ml), followed by SAPE, annexin V, and 7AAD. About 10,000 cells were analyzed and gated for 7AAD-negative (left diagram) and 7AAD-positive cells (right diagram), respectively.

(Fig. 3B, C). TEM of keratinocytes, containing exogenously added A1M and incubated with gold-labeled anti-A1M, showed a highly specific localization of A1M to the mitochondria (Fig. 3C).

Mitochondrial binding was confirmed and the specificity was verified using purified mitochondria from the mouse liver (Fig. 4A). $^{125}$I-labeled A1M was incubated with the mitochondria, with or without an excess of unlabeled A1M or the control protein AGP. Excess of unlabeled A1M blocked the $^{125}$I-A1M binding significantly at the two higher concentrations, whereas AGP at the highest concentration had no effect on the binding. Scatchard analysis of the binding data yielded an affinity constant of the binding at $1.2 \times 10^6\ M^{-1}$.

To investigate if endogenous A1M is found in mitochondria and associated with Complex I, mouse mitochondria were purified without freezing, solubilized, separated under nondenaturing conditions, and analyzed by Western blotting using antibodies against subunits of Complex I and III (denoted NDUFV1and Core I, respectively) and against mouse A1M (Fig. 4B). The results show that A1M co-migrates with

Table 1. $\alpha_1$-Microglobulin-Interacting Proteins Found in the Yeast-Two Hybrid System

| *Protein* | *No. of colonies* | *Genebank Accession No.* | *Bases No.*[a] |
|---|---|---|---|
| NADH dehydrogenase 8-kDa, SDAP subunit (NDUFAB1) | 7 | NM_005003 | 142–670 |
| NADH dehydrogenase 8-kDa, SDAP subunit (NDUFAB1) | 1 | NM_005003 | 18–670 |
| U6 snRNA-associated Sm-like protein (LSM5) | 1 | AF182291 | 14–735 |
| *N*-acetylglucosamine kinase (NAGK) | 1 | AJ242910 | 7–1187 |
| Serologically defined colon cancer antigen 3, NY-CO-3 (SDCCAG3) | 1 | AK001296 | 0–1441 |

[a]According to the base numbering of the Genebank Accession No. assigned in this table.

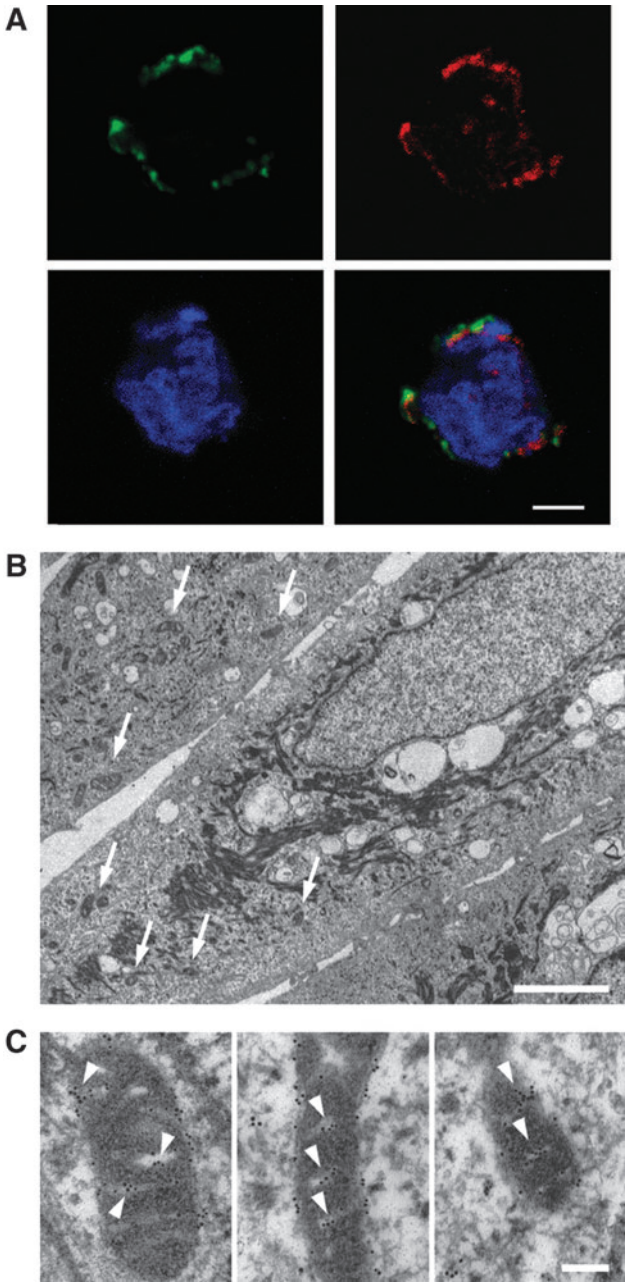


**FIG. 3. Binding of A1M to mitochondria analyzed by confocal microscopy and transmission electron microscopy. (A)** K562 cells incubated with 0.25 mg/ml A1M for 2 h were washed and incubated with MitoTracker (red) for 15 min, and washed in a fresh medium. After washing, cells were then stained with monoclonal mouse anti-A1M (23.26) at 5 $\mu$g/ml, followed by goat anti-mouse IgG F(ab′)$_2$ fragments (Alexa Fluor 488; green). Cells were mounted using ProLong Gold AntiFade Reagent with DAPI (blue). Confocal microscopy was used for analyses as described in the Materials and Methods section. Scale bar indicates 5 $\mu$m. **(B)** An overview of human primary keratinocytes incubated for 20 h at RT with 0.25 mg/ml A1M. Mitochondrial structures are highlighted with *arrows* and shown in higher magnification in **(C)**. Thin sections of human primary keratinocytes were immunolabeled with gold-labeled anti-A1M and shown to correlate to mitochondria. This is highlighted with *arrowheads* **(C)**. The samples were prepared and observed as described in the Materials and Methods section. Scale bar in **(B)** indicates 2 $\mu$m and in **(C)** 0.1 $\mu$m.

the major Complex I-containing band and a supercomplex band containing both Complex I and III, whereas no co-migration was seen between A1M and the major Complex III-containing band. Taken together, this supports a specific association between A1M and a Complex I subunit. However, a large fraction of A1M migrated at a position corresponding to ~200–300 kDa, suggesting that A1M is also associated with other, as yet unidentified, large structures in mitochondria. The blotting intensity of all bands decreased with increasing digitonin concentrations, suggesting that all bands seen in the gels result from noncovalent protein–protein interactions (Supplementary Fig. S1A; Supplementary Data are available online at www.liebertpub.com/ars). The binding between A1M and Complex I was confirmed by anti-Complex I immunoprecipitation followed by blotting with anti-A1M (Fig. 4C). The results show that the majority of A1M-positive bands in the starting material (Fig. 4C, left) were precipitated. Also, a new band, not detectable in the starting material, was seen in the immunoprecipitate. Furthermore, trypsin digestion of intact mitochondria before sodium dodecyl sulfate (SDS)-PAGE and blotting with anti-A1M did not decrease the amount of A1M found in the mitochondria, supporting a localization of A1M in the inner mitochondrial membrane (Supplementary Fig. S1B).

### *A1M protects mitochondrial structure and function*

Hypothesizing that the physiological role of mitochondrial-bound A1M is to confer protection of this organelle against oxidative damage, we first employed TEM to investigate the impact of A1M on the structure of mitochondria in cells exposed to oxidative stress (Fig. 5). TEM was performed on cultured human primary keratinocytes. Extensive destructive effects were seen by heme (Fig. 5B) and $H_2O_2$ (Supplementary Fig. S2B), that is, vast formation of vacuoles, structural disorganization of keratin fibers, and swelling of the mitochondria (Fig. 5B and Supplementary Fig. S2B, zoom). These effects were counteracted by the addition of A1M, where a particular impact was seen on the mitochondrial swelling (Fig. 5C and Supplementary Fig. S2C, zoom). The results suggest that A1M protects and preserves cellular structures otherwise damaged and disintegrated by heme and ROS.

We finally investigated the effects of A1M on mitochondrial function by measuring ATP production of purified mitochondria exposed to heme- or $H_2O_2$-induced oxidative stress (Fig. 6). A significant reduction in the rate of ATP production was seen by 5 and 20 $\mu M$ heme (Fig. 6A). This reduction was reversed by A1M, and no reduction in the ATP production rate was seen by heme in any of the tested concentrations when A1M was present. Similar results were obtained using $H_2O_2$ (Fig. 6B). Thus, $H_2O_2$ significantly reduced the rate of ATP production, but the effects were significantly reversed in the presence of A1M.

## Discussion

In this work, we have shown that the radical scavenger A1M binds to mitochondria and more specifically to mitochondrial Complex I. Furthermore, it was shown that the protein can protect mitochondria from heme- and ROS-induced swelling and loss of ATP production capacity. On the basis of these findings, we suggest a novel cell housekeeping mechanism: regulation of the redox homeostasis of mitochondria by A1M.

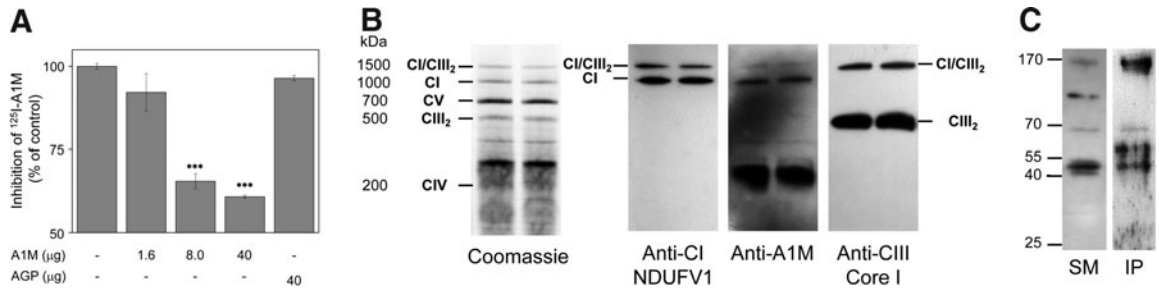


**FIG. 4. Binding of A1M to mitochondria analyzed by $^{125}$I-A1M binding. (A)** The specificity of A1M binding to mitochondria was investigated by mixing ~2.5 $\mu$g/ml of $^{125}$I-A1M with 0.5 mg purified mitochondria in the presence or absence of 1.6–40 $\mu$g of unlabeled protein (A1M or AGP) in phosphate-buffered saline (PBS) + 4% BSA. The mixtures were incubated at 4°C for 30 min, centrifuged on a sucrose gradient to separate unbound protein, and tubes were then frozen, and the cell pellet was cut off and counted in a $\gamma$-counter. Each point represents the mean ± SEM of three determinations. Groups were statistically compared using Student's *t*-test. ***$p < 0.001$. **(B)** The specificity of A1M-binding to mitochondria was further investigated using BN-PAGE and Western blotting. Five $\mu$g mitochondrial membrane proteins from two separate individuals was separated on a BN-PAGE 4%–16% Bis–Tris gel and blotted to a polyvinylidene fluoride (PVDF) membrane. After blocking, the membranes were incubated with antibodies against subunit NDUFV1 of Complex I, mouse A1M, or Core I of Complex III, or stained with Coomassie. **(C)** The Complex I association was also investigated by immunoprecipitation of freshly prepared mitochondria with antibodies against Complex I. After the immunoprecipitation, bound and eluted proteins were separated on a 12% SDS-PAGE and blotted to a PVDF membrane. After blocking, the membranes were incubated with antibodies against mouse A1M. Left lane: mitochondrial starting material (SM) and right lane: bound and eluted material (IP).

The interactions between A1M and mitochondria were observed in several different cell types, that is, human blood cells of lymphocytic, myelocytic, and leukocyte origin, human keratinocytes, and isolated mouse liver mitochondria, suggesting that the interactions and protective effects studied here may be generalized to all types of cells. However, since different cell types have different metabolic and redox conditions, and therefore may behave differently, additional studies are needed to confirm this.

Induction of cell apoptosis was used to mimic situations characterized by stress-induced cell insults causing damage to the plasma membrane and destruction of the external barrier of the cell. Exogenous A1M was bound intracellularly with high affinity as soon as the cells could internalize PI, suggesting that the uptake mechanism is a passive leakage of A1M from the extracellular compartment. Previous studies have shown that the amount of A1M internalized from the extracellular compartment can range between 4% and 18% of the total amount added, suggesting a specific binding and accumulation of A1M in the cells (36, 37). At present, the exact mechanism for the cell uptake is not known nor is the mechanism of the mitochondrial translocation. Previous studies have also shown that the cell uptake of A1M can be increased by alpha-particle irradiation (36). Thus, it can be speculated that ROS and oxidative challenge to cells stimulate the uptake mechanism and upregulate a tentative cellular and/or mitochondrial receptor.

It is becoming increasingly clear that many forms of *in vivo* necrotic cell death actually can be described as a regulated series of ATP-dependent cell disintegration events, that is, programmed necrosis following specific pathways called necroptosis (7, 47). Thus, a possible role for A1M is to participate in preservation of mitochondrial function in both apoptotic and necroptotic cells and possibly other types of necrotic cells during nonautophagic cell death, to ascertain availability of ATP for energy-dependent cell degradation processes. The radical-binding properties of A1M suggest that the protection mechanism is based upon its antioxidant effects, but other mechanisms, such as stabilization of Complex I or the mitochondrial membrane, cannot be ruled out. Furthermore, the mitochondrial electron transport chain is a major source of cellular ROS (6, 27) such as superoxide radicals and $H_2O_2$ formed by Complexes I and III (39, 48). Therefore, an alternative physiological explanation of the localization of A1M to mitochondria is that the protein participates in protection of surrounding tissue components against ROS generated by the mitochondrial respiratory chain during apoptotic or necrotic events in inflammation, infection, or ischemia/reperfusion. In this context, the role of A1M, bound to Complex I, may be to eliminate the ROS before they can participate in unwanted, destructive reactions with healthy tissue. Possibly, A1M fulfills both of these physiological roles *in vivo*: (i) preservation of mitochondrial structure and function and (ii) protection of surrounding tissue from mitochondrial activity.

A1M was found to interact with four different proteins: the NDUFAB1 subunit in the hydrophobic portion of the NADH dehydrogenase complex (46), *N*-acetylglucosamine kinase (18), the snRNA-binding protein LSm5 (41), and a cancer antigen, NY-CO-3 (43). None of the four proteins were a false positive, that is, interacting with the DNA-binding bait fusion protein. Thus, the candidates were regarded as true A1M-interacting proteins in the yeast two-hybrid system. Considering that eight of the 11 clones isolated by the yeast two-hybrid system were the same Complex I subunit, this protein was seen as the most interesting of the proteins and was therefore chosen as a target of further investigations. Since the binding to mitochondria also was supported by alternative methodological approaches and a functional role of the association could be ascribed as compatible with the antioxidation function of A1M, none of the other three A1M-binding proteins have been further investigated in this work. The physiological implications of the binding of A1M to *N*-acetylglucosamine kinase, the snRNA-binding protein LSm5, and NY-CO-3 may be speculated upon, however.

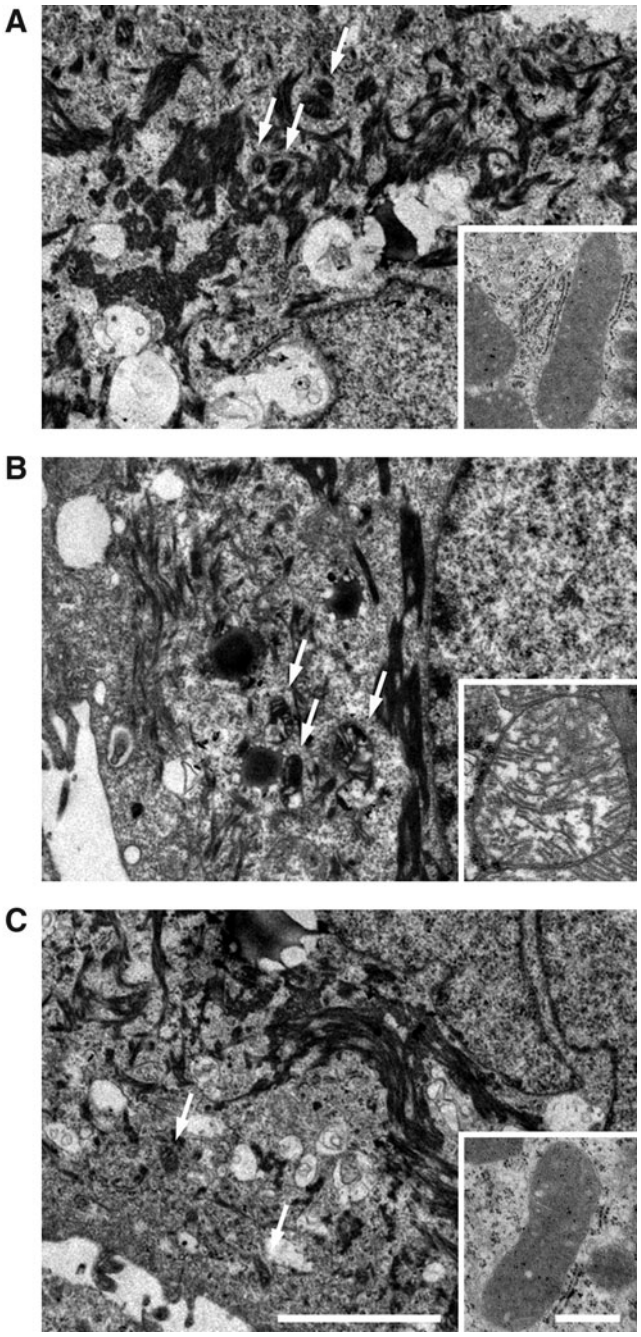


**FIG. 5. A1M protects mitochondrial structure.** Human primary keratinocytes were incubated for 20 h at RT with culture medium only **(A)**, 20 $\mu M$ heme **(B)**, or 20 $\mu M$ heme + 0.25 mg/ml A1M **(C)**. Mitochondrial structures are highlighted with *arrows* and depicted in details (zoomed pictures). The samples were prepared and observed as described in the Materials and Methods section. Scale bar indicates 2 $\mu$m (overview) and 0.1 $\mu$m (zoomed picture).

These proteins are located to the cytosol (19), nucleus (40), and plasma membrane (42), respectively, and the role of the binding to these proteins may be to localize internalized A1M to other cell compartments besides mitochondria. Another possibility is that the binding to these three proteins reflects other functions of A1M unrelated to antioxidation and radical scavenging.

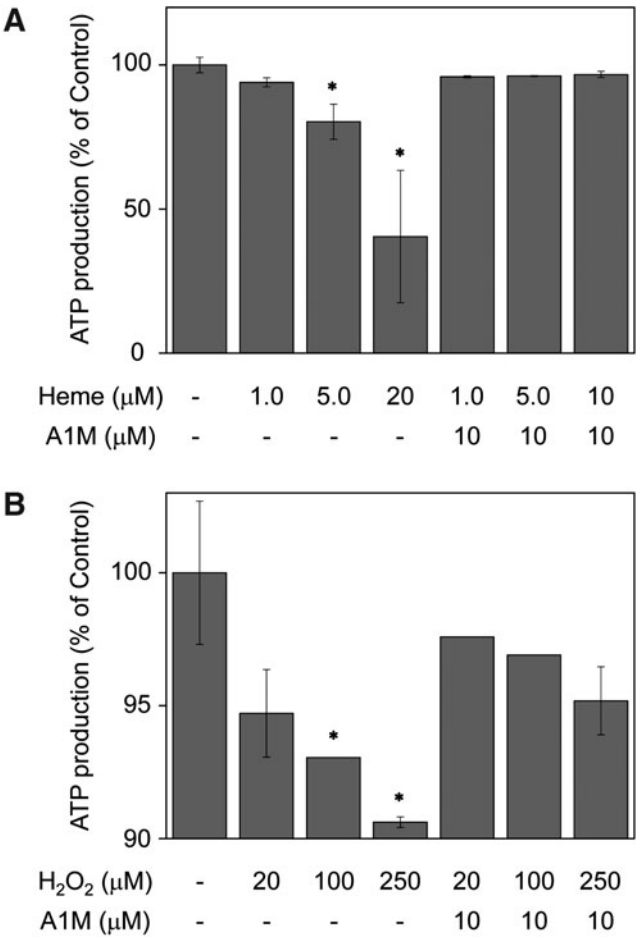


**FIG. 6. A1M protects mitochondrial function.** The effect of A1M on mitochondrial function was investigated by measuring ATP production of purified mitochondria exposed to heme- or hydrogen peroxide ($H_2O_2$)-induced oxidative damage. Mitochondria were incubated with 1–20 $\mu M$ heme, with or without 0.25 mg/ml A1M **(A)**, or 20–250 $\mu M$ $H_2O_2$ with or without 0.25 mg/ml A1M **(B)**, for 30 min. Mitochondria were collected by centrifugation, and ATP production was measured using a luminescence assay kit. ATP levels were normalized to the corresponding sample protein. Each point represents the mean ± SEM of three determinations. Groups were statistically compared using Student's *t*-test. $^*p < 0.05$.

A1M is a member of the Lipocalin protein family. The lipocalins constitute a functionally diverse group of ~50 proteins from bacteria, plants, and animals having an amino acid sequence similarity usually around 20%–25% and share certain structural common features that indicate a common evolutionary origin (11, 12, 1a). Interestingly, two lipocalins found in plants and green algae, violaxanthin de-epoxidase and zeaxtanthin epoxidase, are localized in the thylakoid membranes of chloroplasts, the ATP-producing photosynthetic organelle of plants, where they are associated with the light-harvesting system II and participate in the xanthophyll photoprotection system [reviewed in (14)]. There is an obvious parallel between the violaxanthin protection cycle and the results in this article: the presence of a lipocalin-based protection system in the energy-converting organelles of both plants and animals. In plants, they are believed to have a role in excessive heat dissipation during

light harvesting, and in animal cells, the results in this article suggest that a lipocalin (A1M) participates in maintaining the redox homeostasis of respiration by quenching of the side product ROS. Hypothesizing that mitochondria and chloroplasts have a common prokaryotic or eukaryotic ancestor [*c.f.* (15, 31, 51)], one may speculate that these two lipocalin systems are evolutionarily related.

When a cell is subjected to a fatal insult by, for instance, oxidation, it will ultimately be degraded and its components recycled. Preservation and maintenance of the mitochondrial energy machinery during this process are vital. In this article, we have shown that the reductase and radical scavenger A1M may have a central role in maintaining mitochondrial energy production. It can be speculated that A1M at the same time may counteract and eliminate the ROS generated in the respiratory chain to prevent unwanted, destructive reactions with healthy tissue, which is in line with its previously reported capacity to prevent ROS-induced cell and tissue damage (2, 32–34, 36, 37, 1c). Thus, these findings suggest a novel mechanism of maintaining mitochondrial redox homeostasis.

## Materials and Methods

### *Proteins and antibodies*

Human monomeric plasma A1M was isolated by anti-A1M affinity chromatography and Sephacryl S-300 gel-chromatography, as described previously (49). Recombinant human A1M, containing an N-terminal His-tag, was purified from the culture medium of baculovirus-infected insect cells (49) or expressed in *Escherichia coli* and purified and refolded as described (21, 33). Human serum AGP and ovalbumin were purchased from Sigma-Aldrich Co., and BSA was from Roche Diagnostics Scandinavia AB. Hemin (Ferriprotoporphyrin IX chloride) was purchased from Porphyrin Products, Inc., and a 10 m*M* stock solution was prepared fresh by dissolving in DMSO (Sigma-Aldrich). $H_2O_2$ was from Acros Organics. Mouse monoclonal antibodies against human A1M (BN11.3 and 23.26) were raised as described (30). Rabbit polyclonal anti-mouse A1M antibodies (Sven; IgG-fraction) were prepared as described (42). The hamster anti-mouse CD3 antibody (145.2C11) was kindly provided by Dr. Rikard Holmdahl, Lund University. Fluorescein isothiocyanate-conjugated goat anti-mouse immunoglobulin (GAM-FITC) and phycoerythrin-conjugated streptavidin (SAPE) were purchased from DAKO A/S, and 7 AAD was from Sigma-Aldrich Co., and annexin V-FITC was from Trevigen, Inc.

### *Cell culture*

A mouse CD4+ T-cell hybridoma cell line (HCQ.4), 70Z/3, K562, and human primary keratinocytes (Cambrex Biologics) were employed for studies on A1M binding to cells and mitochondria. Cells were cultivated as described previously (26, 29, 38) and processed and analyzed as described below.

### *Induction of apoptosis*

Apoptosis was induced in the T-cell hybridoma by three different treatments: Cells were incubated on anti-CD3 antibody-coated plastics (4 $\mu$g/ml) (44), or incubated in a medium supplemented with either 5% ethanol or 10% of DMSO (25). Apoptosis was detected as DNA fragmentation by agarose gel electrophoresis (described below), and cell viability was measured by trypan blue exclusion. In the pre-B-cell line, apoptosis was induced by the 3-CPA (Oxigene, Inc.) as described in (26).

### *Agarose electrophoresis*

To detect DNA fragmentation, $\sim 1 \times 10^6$ cells were lysed, proteinase K- and RNAse A-treated, and analyzed by agarose electrophoresis.

### *Labeling of A1M*

For analysis of A1M binding to cells, A1M was biotinylated, FITC-conjugated, or radiolabeled with $^{125}$I as described previously (9, 13, 16).

### *Flow cytometry*

A1M binding to cells was analyzed by flow cytometry. Approximately $1 \times 10^6$ cells were analyzed for A1M binding in one of three different ways: (i) The cells were incubated with 1 mg/ml of plasma or recombinant insect cell A1M, followed by 10 $\mu$g/ml of monoclonal mouse anti-A1M (BN 11.3) and GAM-FITC (diluted 20 times). (ii) The cells were incubated with 10 $\mu$g/ml biotinylated A1M followed by SAPE (diluted according to the manufacturer's recommendations). (iii) The cells were incubated with 0.1 mg/ml FITC-conjugated A1M. All incubations were performed in phosphate-buffered saline (PBS) + 1 mg/ml of BSA for 10 min at room temperature (RT). Between the incubations, the cells were washed 2–3 times in PBS. To detect leaking cells, cells were incubated with PI (Invitrogen, Inc.) or 7AAD (according to manufacturers' instructions). To detect apoptotic 70Z/3 cells, cells were also incubated with FITC-conjugated annexin V in a $Ca^{2+}$-containing buffer (according to the manufacturers' instructions). A Becton Dickinson FACSorter and the Cell Quest software package were used for all analyses.

### *Fluorescence and confocal microscopy*

K562 cells were washed and resuspended in the culture medium to $0.5–4.0 \times 10^6$ cells/ml and incubated with or without A1M as indicated in the figure legends. Cells were then either incubated with MitoTracker (Invitrogen, Inc.) for 15 min at 37°C and washed in a fresh medium (Fig. 3A) or directly washed in a fresh medium (Fig. 1D). Cells were then resuspended in an ice-cold Na-medium (5.4 m*M* KCl; 1.2 m*M* $KH_2PO_4$; 0.8 m*M* $MgSO_4$; 5.6 m*M* D-glucose; 127 m*M* NaCl; 10 m*M* Hepes; 1.8 m*M* $CaCl_2$; pH 7.3), followed by fixation with 1% BD CellFIX on ice for 15 min and at RT for 45 min. Cells were then washed in a blocking solution (Na-medium; 1% BSA; 5% goat serum) followed by permeabilization in 0.02% Triton-X and blocking in 1% BSA, 5% goat serum, and 0.2% Tween-20 for 1 h at RT. The cells were then incubated overnight with monoclonal mouse anti-A1M (23.26) at 5 $\mu$g/ml, at 4°C. Subsequently, goat anti-mouse IgG F(ab')$_2$ fragments conjugated with Alexa Fluor® 488 (Invitrogen, Inc.) was applied for 1 h at RT. Cells were mounted using ProLong Gold AntiFade Reagent containing 4',6-diamidino-2-phenylindole

(DAPI; Invitrogen, Inc.). Cells and fluorescent markers were analyzed using an epifluorescence microscope (Nikon Eclipse TE300) and a confocal laser-scanning microscope (Zeiss LSM 510 Meta). The epifluorescence microscope was equipped with the appropriate filter combinations to selectively visualize the used fluorophores. A Plan Apochromat 100× lens was used for analyses, and the image data were collected with a Hamamatsu C4742-95 CCD camera. To analyze intracellular labeling and colabeling in subcellular structures, confocal scanning of optical sections was recorded through the cells. For excitation of the fluorophores, the 405-nm laser line was used for DAPI (diode laser 405–30); the 488-nm laser line was used for Alexa Fluor 488 (Argon laser), and the 561-nm laser line was used for MitoTracker (DPSS 561-10). The individual fluorophore emission wavelengths were detected using the following filters: band-pass 420–480 nm for DAPI, band-pass 505–550 nm for Alexa Fluor 488, and long-pass 575 nm for MitoTracker. The pinhole for detection of Alexa Fluor 488 (488-nm excitation) was set to correspond to 1 (one) Airy unit, and the pinholes for the other detection channels were then adjusted to give optical sections of the same thickness, that is, to ensure comparisons of the corresponding confocal volumes. Laser power and detection settings (gain and offset) were optimized for the individual channels, giving a detection range from highly saturated pixels of larger structures to nonsaturated pixels of small structures. The different fluorophores were sequentially scanned, that is, with optimal settings for one fluorophore in each channel, at a 512×512 or 1024×1024 frame size. To determine cellular morphology, differential interference contrast images were obtained using the 405-nm laser as transmitted light. The spatial relation between the Alexa Fluor 488 fluorescence (green) and MitoTracker fluorescence (red) was determined *via* merging of the optical sections from the individually scanned channels (yellow when colocalized), confirmed *via* analyses of merged images using LSM Zen software (Profile, data not shown).

### *Yeast two-hybrid system*

A GAL4-based yeast two-hybrid system was used to search for A1M-interacting cellular proteins. DNA encoding the A1M part (amino acids 1–183) of the A1M-bikunin gene (*AMBP*) was amplified by PCR using a pCR-Script construct as a template. The fragment was completely sequenced and ligated into the yeast two-hybrid vector pBD-GAL4 Cam phagemid vector (Stratagene). The recombinant vector was then transformed into the *Saccharomyces cerevisiae* yeast host strain (YRG-2; Stratagene). The yeast strains were grown and maintained and two-hybrid assays were performed using standard protocols as recommended by Stratagene and www.umanitoba.ca/faculties/medicine/units/biochem/gietz/. Approximately $7.5\times10^8$ YRG-2 carrying the bait plasmid, pBD-GAL4-A1M, were transformed with 15–20 $\mu$g of a human leukocyte MATCHMAKER cDNA library (Clontech Laboratories, Inc.). The resulting $\sim2\times10^6$ transformants were analyzed by histidine prototrophy assay and $\beta$-gal colony-lift assay. Recombinant library plasmids from the $His^+LacZ^+$ transformants were isolated and retested in direct two-hybrid assays together with the A1M bait plasmid as well as with bait plasmids encoding unrelated proteins. Plasmids resulting in activation of the reporter genes together with the A1M-encoding bait plasmid, but not with the bait plasmids encoding unrelated proteins, were regarded as true positives. The DNA sequence of the inserts was determined using the vector primers pAD5′: 5′-TCCAGATT ACGCTAGCTTGGGTGGTCATATG-3′ and pAD3′: 5′-GTGAA CTTGCGGGGTTTTTCAGTATCTACGA-3′. One of the inserts was sequenced completely by Innovagen AB.

### *Mitochondrial preparation from mouse liver tissue*

Mouse liver tissue was collected in an ice-cold isolation buffer (320 m*M* sucrose, 10 m*M* Trizma Base, and 2 m*M* EGTA) and subsequently homogenized in 2 ml homogenization buffer (isolation buffer supplemented with 1% BSA). Mitochondria were prepared from homogenates by sequential centrifugation, including density purification on 19% Percoll. The protein concentration of mitochondrial preparations was determined using Nanodrop, and isolated mitochondria were used without freezing.

### *Competitive cell- and mitochondrion-binding assay*

The specificity of A1M binding to cells and mitochondria was investigated by a competitive cell-binding assay as described (3, 50). Apoptosis was induced in HCQ.4 cells by anti-CD3 cross-linking for 15–18 h. The cells were harvested and compared to normal cells in the binding assay. A1M, ovalbumin, BSA, and AGP diluted in PBS + 2% BSA were used as unlabeled control proteins. An affinity constant for the binding was calculated using a Scatchard plot of the data.

### *Immunocapture of Complex I*

Complex I was immunoprecipitated on freshly prepared mitochondria using the Complex I Immunocapture Kit (MitoSciences). After the immunoprecipitation, bound proteins were eluted using the SDS buffer and subsequently analyzed using SDS-PAGE and Western blotting.

### *Isolation of respiratory chain complexes and supercomplexes*

Freshly isolated, nonfrozen mitochondria were suspended in PBS supplemented with a Complete Mini-Protease inhibitor. Mitochondria were pelleted for 5 min at 5000 *g* and subsequently dissolved to a concentration of 5 mg/ml in the MB2 buffer (1.75 *M* aminocaproic acid, 7.5 m*M* Bis–Tris, pH 7.0, +2 m*M* EGTA, pH 8.0). Mitochondrial membrane proteins were solubilized by incubation with 0.5 g digitonin/g protein for 5 min on ice. Samples were centrifuged for 30 min at 13000 *g*; the supernatant was collected and the protein concentration measured as before. Finally, SBG (750 m*M* aminocaproic acid and 5% Serva Blue G) was added to a final concentration of 4.5%.

### *Blue native PAGE, SDS-PAGE, and Western blotting*

Five $\mu$g mitochondrial membrane proteins was separated on a BN-PAGE 4%–16% Bis–Tris gel and either stained with Coomassie Brilliant Blue or blotted to a polyvinylidene fluoride (PVDF) membrane. Complex I immunoprecipitated proteins were separated on a 12% SDS-PAGE and transferred to a PVDF membrane. After blocking, the membranes were incubated with antibodies detecting Complex I subunit NDUFV1 (Sigma), Complex III subunit Core I (Invitrogen,

Inc.), or mouse A1M (Sven). Primary antibodies were detected by incubation with horseradish peroxidase-coupled goat anti-mouse (DAKO) or goat anti-rabbit (DAKO).

### *Transmission electron microscopy*

Human keratinocytes (about 1 million cells), incubated for 20 h at RT with 20 $\mu M$ heme, with or without 0.25 mg/ml A1M, were pelleted by centrifugation and prepared as previously described (33). Thin sections with gold-labeled anti-A1M (BN11.3) were immunolabeled as described previously (40), with the modification that Aurion-BSA was used as a blocking agent. Specimens were observed in a JEOL JEM 1230 electron microscope operated at an 80-kV accelerating voltage. Images were recorded with a Gatan Multiscan 791 CCD camera.

### *ATP assay*

Cellular ATP production was measured using a luminescence assay kit (Promega), based on the ATP-dependent activity of luciferase. ATP levels were normalized to the corresponding sample protein content.

### *Statistical analysis*

Origin 8 software was used for statistical analysis. Student's *t*-test was used for statistical evaluation and was considered significant when $p < 0.05$.

## Acknowledgments

This work was supported by the Swedish Research Council, governmental ALF research grants to Lund University and Lund University Hospital, the Swedish Cancer Foundation, the Royal Physiographic Society in Lund, the Foundations of Greta and Johan Kock and Alfred Österlund, the Blood and Defence Network, Lund University, and A1M-Pharma AB. The authors wish to acknowledge Maria Baumgarten for outstanding electron microscopy work, Dr. Ulrich von Pawel-Rammingen for kindly donating the human leukocyte library and for fruitful discussions, Drs. Christine Persson and Kurt Schesser for fruitful discussions, and Eva Miller, Kerstin Torrikka, Kerstin Boll, Lisa Palm, Jenny Johansson, and Eva Hansson for excellent technical assistance. We are grateful to Dr. Bo Holmqvist, ImaGene-iT AB (Medicon Village, Lund, Sweden), for help with the confocal microscopy.

The authors MGO and BÅ are cofounders of the company A1M Pharma AB. This does not present any conflict of interest.

## Author Disclosure Statement

No competing financial interests exist.

## References

1a. Åkerström B, Flower DR, and Salier JP. Lipocalins: unity in diversity. *Biochim Biophys Acta* 1482: 1–8, 2000.

1b. Åkerström B and Lögdberg L. $\alpha_1$-microglobulin. In: *Lipocalins*, edited by Åkerström B, Borregaard N, Flower DR, and Salier J-P. Georgetown, TX: Landes Bioscience, 2006. pp. 110–120.

1c. Åkerström B, Maghzal GJ, Winterbourn CC, and Kettle AJ. The lipocalin $\alpha_1$-microglobulin has radical scavenging activity. *J Biol Chem* 282: 31493–31503, 2007.

1d. Allhorn M, Berggård T, Nordberg J, Olsson ML, and Åkerström B. Processing of the lipocalin $\alpha_1$-microglobulin by hemoglobin induces heme-binding and heme-degradation properties. *Blood* 99: 1894–1901, 2002.

2. Allhorn M, Klapyta A, and Åkerström B. Redox properties of the lipocalin $\alpha_1$-microglobulin: reduction of cytochrome c, hemoglobin, and free iron. *Free Radic Biol Med* 38: 557–567, 2005.

3. Babiker-Mohamed H, Olsson ML, Boketoft A, Lögdberg L, and Åkerström B. $\alpha_1$-microglobulin is mitogenic to human peripheral blood lymphocytes. Regulation by both enhancing and suppressive serum factors. *Immunobiology* 180: 221–234, 1990.

4. Berggård T, Oury TD, Thogersen IB, Åkerström B, and Enghild JJ. $\alpha_1$-microglobulin is found both in blood and in most tissues. *J Histochem Cytochem* 46: 887–894, 1998.

5. Berggård T, Thelin N, Falkenberg C, Enghild JJ, and Åkerström B. Prothrombin, albumin and immunoglobulin A form covalent complexes with $\alpha_1$-microglobulin in human plasma. *Eur J Biochem* 245: 676–683, 1997.

6. Brand MD. The sites and topology of mitochondrial superoxide production. *Exp Gerontol* 45: 466–472, 2010.

7. Degterev A and Yuan J. Expansion and evolution of cell death programmes. *Nat Rev Mol Cell Biol* 9: 378–390, 2008.

8. DeMars DD, Katzmann JA, Kimlinger TK, Calore JD, and Tracy RP. Simultaneous measurement of total and IgA-conjugated $a_1$-microglobulin by a combined immunoenzyme/immunoradiometric assay technique. *Clin Chem* 35: 766–772, 1989.

9. Elbashir MI, Nilson BH, Åkesson P, Björck L, and Åkerström B. Antibody response in immunized rabbits measured with bacterial immunoglobulin-binding proteins. *J Immunol Methods* 135: 171–179, 1990.

10. Faivre B, Menu P, Labrude P, and Vigneron C. Hemoglobin autooxidation/oxidation mechanisms and methemoglobin prevention or reduction processes in the bloodstream. Literature review and outline of autooxidation reaction. *Artif Cells Blood Substit Immobil Biotechnol* 26: 17–26, 1998.

11. Flower DR. The lipocalin protein family: structure and function. *Biochem J* 318 (Pt 1): 1–14, 1996.

12. Ganfornina L, Sanchez D, Greene LH, and Flower DR. The lipocalin protein family. Protein sequence, structure and relationship to calycin superfamily. In: *Lipocalins*. edited by Åkerström B, Borregaard N, Flower DR and Salier JP. Georgetown, TX.: Landes Bioscience; 2006. pp. 17–27.

13. Goding JW. *Monoclonal Antibodies: Principles and Practice.* Orlando, FL: Academic Press, 1986.

14. Goss R and Jakob T. Regulation and function of xanthophyll cycle-dependent photoprotection in algae. *Photosynth Res* 106: 103–122, 2010.

15. Gray MW, Burger G, and Lang BF. Mitochondrial evolution. *Science* 283: 1476–1481, 1999.

16. Greenwood FC, Hunter WM, and Glover JS. The Preparation of I-131-Labelled Human Growth Hormone of High Specific Radioactivity. *Biochem J* 89: 114–123, 1963.

17. Halliwell B and Gutteridge JM. *Free Radicals in Biology and Medicine.(4th ed)* Oxford: Oxford University Press, 2007.

18. Hinderlich S, Berger M, Schwarzkopf M, Effertz K, and Reutter W. Molecular cloning and characterization of murine and human N-acetylglucosamine kinase. *Eur J Biochem* 267: 3301–3308, 2000.

19. Hinderlich S, Nohring S, Weise C, Franke P, Stasche R, and Reutter W. Purification and characterization of N-acetylglucosamine kinase from rat liver—comparison with UDP-N-acetylglucosamine 2-epimerase/N-acetylmannosamine kinase. *Eur J Biochem* 252: 133–139, 1998.
20. Kastern W, Björck L, and Åkerström B. Developmental and tissue-specific expression of $\alpha_1$-microglobulin mRNA in the rat. *J Biol Chem* 261: 15070–15074, 1986.
21. Kwasek A, Osmark P, Allhorn M, Lindqvist A, Åkerström B, and Wasylewski Z. Production of recombinant human alpha1-microglobulin and mutant forms involved in chromophore formation. *Protein Expr Purif* 53: 145–152, 2007.
22. Larsson J, Allhorn M, and Åkerström B. The lipocalin $\alpha_1$-microglobulin binds heme in different species. *Arch Biochem Biophys* 432: 196–204, 2004.
23. Larsson J, Wingårdh K, Berggård T, Davies JR, Lögdberg L, Strand SE, and Åkerström B. Distribution of iodine $^{125}$-labeled $\alpha_1$-microglobulin in rats after intravenous injection. *J Lab Clin Med* 137: 165–175, 2001.
24. Lee J, Giordano S, and Zhang J. Autophagy, mitochondria and oxidative stress: cross-talk and redox signalling. *Biochem J* 441: 523–540, 2012.
25. Lennon SV, Martin SJ and Cotter TG. Dose-dependent induction of apoptosis in human tumour cell lines by widely diverging stimuli. *Cell Prolif* 24: 203–214, 1991.
26. Liberg D, Lazarevic B, Pero RW, and Leanderson T. N-substituted benzamides inhibit NFkappaB activation and induce apoptosis by separate mechanisms. *Br J Cancer* 81: 981–988, 1999.
27. Loschen G, Azzi A, and Flohe L. Mitochondrial H2O2 formation: relationship with energy conservation. *FEBS Lett* 33: 84–87, 1973.
28. May K, Rosenlöf L, Olsson MG, Centlow M, Mörgelin M, Larsson I, Cederlund M, Rutardóttir S, Siegmund W, Schneider H, Åkerström B, and Hansson SR. Perfusion of human placenta with hemoglobin introduces preeclampsia-like injuries that are prevented by $\alpha_1$-microglobulin. *Placenta* 32: 323–332, 2011.
29. Michaelsson E, Malmström V, Reis S, Engström A, Burkhardt H, and Holmdahl R. T cell recognition of carbohydrates on type II collagen. *J Exp Med* 180: 745–749, 1994.
30. Nilson B, Åkerström B, and Lögdberg L. Cross-reacting monoclonal anti-$\alpha_1$-microglobulin antibodies produced by multi-species immunization and using protein G for the screening assay. *J Immunol Methods* 99: 39–45, 1987.
31. Nisbet EG and Sleep NH. The habitat and nature of early life. *Nature* 409: 1083–1091, 2001.
32. Olsson MG, Allhorn M, Bulow L, Hansson SR, Ley D, Olsson ML, Schmidtchen A, and Åkerström B. Pathological conditions involving extracellular hemoglobin: molecular mechanisms, clinical significance, and novel therapeutic opportunities for $\alpha_1$-microglobulin. *Antioxid Redox Signal* 17: 813–846, 2012.
33. Olsson MG, Allhorn M, Larsson J, Cederlund M, Lundqvist K, Schmidtchen A, Sorensen OE, Mörgelin M, and Åkerström B. Up-regulation of A1M/$\alpha_1$-microglobulin in skin by heme and reactive oxygen species gives protection from oxidative damage. *PLoS One* 6: e27505, 2011.
34. Olsson MG, Allhorn M, Olofsson T, and Åkerström B. Up-regulation of $\alpha_1$-microglobulin by hemoglobin and reactive oxygen species in hepatoma and blood cell lines. *Free Radic Biol Med* 42: 842–851, 2007.
35. Olsson MG, Centlow M, Rutardóttir S, Stenfors I, Larsson J, Hosseini-Maaf B, Olsson ML, Hansson SR, and Åkerström B. Increased levels of cell-free hemoglobin, oxidation markers, and the antioxidative heme scavenger $\alpha_1$-microglobulin in preeclampsia. *Free Radic Biol Med* 48: 284–291, 2010.
36. Olsson MG, Nilsson EJ, Rutardottir S, Paczesny J, Pallon J, and Åkerström B. Bystander cell death and stress response is inhibited by the radical scavenger $\alpha_1$-microglobulin in irradiated cell cultures. *Radiat Res* 174: 590–600, 2010.
37. Olsson MG, Olofsson T, Tapper H, and Åkerström B. The lipocalin $\alpha_1$-microglobulin protects erythroid K562 cells against oxidative damage induced by heme and reactive oxygen species. *Free Radic Res* 42: 725–736, 2008.
38. Paige CJ, Kincade PW, and Ralph P. Murine B cell leukemia line with inducible surface immunoglobulin expression. *J Immunol* 121: 641–647, 1978.
39. Poyton RO, Ball KA, and Castello PR. Mitochondrial generation of free radicals and hypoxic signaling. *Trends Endocrinol Metab* 20: 332–340, 2009.
40. Roth J. Post-embedding cytochemistry with gold-labelled reagents: a review. *J Microsc* 143: 125–137, 1986.
41. Salgado-Garrido J, Bragado-Nilsson E, Kandels-Lewis S, and Seraphin B. Sm and Sm-like proteins assemble in two related complexes of deep evolutionary origin. *EMBO J* 18: 3451–3462, 1999.
42. Sanchez D, Martinez S, Lindqvist A, Åkerström B, and Falkenberg C. Expression of the AMBP gene transcript and its two protein products, $\alpha_1$-microglobulin and bikunin, in mouse embryogenesis. *Mech Dev* 117: 293–298, 2002.
43. Scanlan MJ, Chen YT, Williamson B, Gure AO, Stockert E, Gordan JD, Tureci O, Sahin U, Pfreundschuh M, and Old LJ. Characterization of human colon cancer antigens recognized by autologous antibodies. *Int J Cancer* 76: 652–658, 1998.
44. Shi YF, Szalay MG, Paskar L, Sahai BM, Boyer M, Singh B, and Green DR. Activation-induced cell death in T cell hybridomas is due to apoptosis. Morphologic aspects and DNA fragmentation. *J Immunol* 144: 3326–3333, 1990.
45. Tejler L, Eriksson S, Grubb A, and Astedt B. Production of protein HC by human fetal liver explants. *Biochim Biophys Acta* 542: 506–514, 1978.
46. Triepels R, Smeitink J, Loeffen J, Smeets R, Buskens C, Trijbels F, and van den Heuvel L. The human nuclear-encoded acyl carrier subunit (NDUFAB1) of the mitochondrial complex I in human pathology. *J Inherit Metab Dis* 22: 163–173, 1999.
47. Vandenabeele P, Galluzzi L, Vanden Berghe T, and Kroemer G. Molecular mechanisms of necroptosis: an ordered cellular explosion. *Nat Rev Mol Cell Biol* 11: 700–714, 2010.
48. Weisiger RA and Fridovich I. Mitochondrial superoxide simutase. Site of synthesis and intramitochondrial localization. *J Biol Chem* 248: 4793–4796, 1973.
49. Wester L, Johansson MU, and Åkerström B. Physicochemical and biochemical characterization of human $\alpha_1$-microglobulin expressed in baculovirus-infected insect cells. *Protein Expr Purif* 11: 95–103, 1997.
50. Wester L, Michaelsson E, Holmdahl R, Olofsson T, and Åkerström B. Receptor for $\alpha_1$-microglobulin on T lymphocytes: inhibition of antigen-induced interleukin-2 production. *Scand J Immunol* 48: 1–7, 1998.
51. Xiong J, Fischer WM, Inoue K, Nakahara M, and Bauer CE. Molecular evidence for the early evolution of photosynthesis. *Science* 289: 1724–1730, 2000.

Address correspondence to:
*Dr. Magnus G. Olsson*
*Division of Infection Medicine*
*Lund University*
*BMC B14*
*Lund 221 84*
*Sweden*

*E-mail:* magnus.gram@med.lu.se

Date of first submission to ARS Central, April 23, 2012; date of final revised submission, November 05, 2012; date of acceptance, November 18, 2012.

**Abbreviations Used**

3-CPA = benzamide drug declopramide
7 AAD = 7-amino actinomycin D
70Z/3 = murine pre-B-cell line
A1M = $\alpha_1$-microglobulin
AGP = $\alpha_1$-acid glycoprotein
*AMBP* = *A1M-Bikunin gene*
BSA = bovine serum albumin
DAPI = 4′-6-diamidino-2-phenylindole
DIC = differential interference contrast
DMSO = dimethyl sulfoxide
GAM-FITC = fluorescein isothiocyanate-conjugated goat anti-mouse immunoglobulin
$H_2O_2$ = hydrogen peroxide
Hb = hemoglobin
HCQ.4 = murine T-cell hybridoma cell line
$Hiz^+LacZ^+$ = histidine and $\beta$-galactosidase positive
K562 = human erythroid cell line
LSm5 = U6 snRNA-associated Sm-like protein
NAGK = *N*-acetylglucosamine kinase
NDUFAB1 = NADH dehydrogenase 8-kDa, SDAP subunit
PAGE = polyacrylamide gel electrophoresis
PBS = phosphate-buffered saline
PI = propidium iodide
PVDF = polyvinylidene fluoride
ROS = reactive oxygen species
SAPE = phycoerythrin-conjugated streptavidin
SDCCAG3/NY-CO-3 = serologically defined colon cancer antigen 3
SDS = sodium dodecyl sulfate
snRNA = small nuclear RNA
TEM = transmission electron microscopy
YRG-2 = *Saccharomyces cerevisiae* yeast host strain
ZDE = zeaxanthin epoxidase